Surface Science 605 (2011) 1791–1796

Contents lists available at ScienceDirect

Surface Science

journal homepage: www.elsevier.com/ locate/susc

X-ray scattering study of interfacial roughness in Nb/PdNi multilayers

A. Vecchione [a,*], R. Fittipaldi [a], C. Cirillo [a], M. Hesselberth [b], J. Aarts [b], S.L. Prischepa [c], V.N. Kushnir [c], M.Yu. Kupriyanov [d], C. Attanasio [a]

[a] CNR-SPIN Salerno and Dipartimento di Fisica "E.R. Caianiello" Università degli Studi di Salerno, Fisciano (Sa) I-84084, Italy
[b] Kamerlingh Onnes Laboratory, Leiden University, P.O. Box 9504, 2300 RA Leiden, The Netherlands
[c] Belarus State University of Informatics and Radioelectronics, P. Browka 6, Minsk 220013, Belarus
[d] Institute of Nuclear Physics, Moscow State University, Moscow 119992, Russia

ARTICLE INFO

Article history:
Received 3 May 2011
Accepted 9 June 2011
Available online 16 June 2011

Keywords:
Specular X-ray scattering
Diffuse X-ray scattering
Interfacial roughness
Metallic multilayers
X-ray reflectivity
Correlated roughness
Superconductivity
Ferromagnetism

ABSTRACT

Specular and diffuse X-ray scattering are used to study interfacial roughness in $Nb/Pd_{0.81}Ni_{0.19}$ multilayers deposited by dc UHV sputtering. The data are analyzed to extract information about the correlated behavior of interface roughness in both the lateral and vertical directions. X-ray reflectivity is treated quantitatively by computer-aided simulation and modelling in order to extract values also for the layers thickness. From the analysis of the diffusive spectra of the reflectivity maps the roughness correlation has been evaluated.

© 2011 Elsevier B.V. All rights reserved.

1. Introduction

In recent years much activity has been devoted to the study of the interplay between superconductivity (S) and ferromagnetism (F) in artificial S/F hybrids in which these two antagonistic orderings are present in spatially separated layers, interacting via the proximity effect [1,2]. Such great interest is due to the peculiar effects emerging from the inhomogeneous nature of the superconducting order parameter induced in the F layer. Signatures of this inhomogeneous state are: nonmonotonic dependence of the superconducting transition temperature as a function of the ferromagnetic layer thickness, $T_c(d_F)$, (for an exhaustive review see [3]), nonmonotonic behavior of the anisotropy coefficient in S/F/S trilayers [4], negative critical current [5,6] and reversed density of states [7] in Josephson and tunnel S/F/S π-junctions. At the beginning of this research the experimental investigation was performed on S/F multilayers [3,8–11]. However, also due to the lack of sample reproducibility, the results of the measurements were often not conclusive and a clear comparison between the theoretical predictions and the experimental results could be controversial [12–14]. Even correlations between the observed $T_c(d_F)$ dependencies and the preparation methods (Molecular Beam Epitaxy or sputtering technique) were suggested [3,15]. Nowadays, it is well known that the superconducting properties of S/F hybrids are strongly influenced by certain aspects of their structure, for example the thickness control of each layer [16,17], the flatness [18–20], and the presence of alloying or interdiffusion at the interfaces [21,22]. Fortunately, the continuous developments in the fabrication techniques made recently possible the reliable realization of complex heterostructures consisting of layers of different materials only few nanometers thick, coupled through high-quality contacts. Lately, even so called stepped 0–π Josephson junctions, namely junctions with a tailored step in the thickness of the ferromagnetic layer, were successfully fabricated [23]. Very recently a complex multilayered structure consisting of up to more than ten single layers has been employed to observe spin-triplet superconductivity in ferromagnetic Josephson junctions [24,25]. These technological progresses are crucial, since the peculiar effects related to the S/F coexistence are observable in a narrow range of ferromagnetic thickness of a few nanometers, where structural and magnetic properties are also critical. Due to the small ferromagnetic thickness required in these structures, in fact, the thickness and the roughness of these layers has to be controlled on a sub-nanometer scale. It has been demonstrated that, for instance, small fluctuation in the layers parameter, especially in the region where the π-phase takes place, could affect the shape of the resistive transitions of S/F/S trilayers [26–28]. Moreover, study of interfaces between metals or oxides is important in view of modification of ultra-thin films grown on different templates [29] and for optimizing the low-dimensional devices [30,31]. For all these reasons the preparation of high-quality multilayers should be

* Corresponding author.
E-mail address: vecchione@sa.infn.it (A. Vecchione).

0039-6028/$ – see front matter © 2011 Elsevier B.V. All rights reserved.
doi:10.1016/j.susc.2011.06.013

Библиотека БГУИР

supported by a robust characterization of these key physical parameters. In this sense X-ray Reflectivity (XRR) provides a nondestructive and accurate characterization of thin films and multilayers. XRR probes the intensity of scattered X-rays at small angles, providing information about film thickness, roughness, and density. These analyses, pursued for the case of S/N systems (here N stands for normal metal) [32–34], is lacking in the case of S/F ones. To our knowledge XRR has been employed on hybrid S/F structures only in the specular condition, to evaluate the thickness and the roughness of the layers [9,11,13–15,35–38]. Occasionally Rutherford Backscattering analysis (RBS) has been also used to determine the layers thickness [15–17] with no particular focus, however, on the elemental area density or impurity distribution. We believe that a more systematic study of the structural properties of heterostructures employed in experiments aimed at the investigation of the interplay between superconductivity and magnetism is fundamental.

In this paper X-Ray reflectivity (XRR) has been employed in the characterization of a series of high-quality superconducting Nb/$Pd_{0.81}Ni_{0.19}$(PdNi) multilayers (containing up to nineteen single layers) deposited by dc UHV-sputtering. Reflectivity data are treated quantitatively by computer-aided simulation and modeling in order to extract values for the interface roughness and the layers thickness. From the analysis of the diffusive spectra of the reflectivity maps also the roughness correlation has been evaluated.

2. Fabrication and preliminary characterization of the multilayers

2.1. Growth of Nb/PdNi multilayers

The samples consist of weakly ferromagnetic PdNi and superconducting Nb layers. The Nb/PdNi multilayers analyzed in this work have the following structure: Si/(PdNi/Nb)$_{\times m}$/PdNi, where m is the number of bilayers in the stack. The samples have nominal Nb and PdNi layers thickness of $d_{Nb}=190$ Å and $d_{PdNi}=20$ Å, while different for the number of bilayers, $m=5$, 7, 9. In the following we will call these samples KL5, KL7, and KL9, respectively. The PdNi cap layer has the same nominal thickness of the internal one. Great care was paid to samples fabrication in order to provide identical deposition conditions for all the multilayers in the series. This concern pertains in particular to the quality of the interfaces and of the layering, as well as to the thickness control through the whole structures. The multilayers were deposited by dc magnetron sputtering on Si(100) substrates at room temperature. The sputtering is a multi-target UHV vacuum system, equipped with a load-lock chamber. The base pressure in the main chamber was in the 10^{-10} mbar range. The load-lock, with a base pressure of the order of 10^{-8} mbar, can house up to 6 substrates. In each deposition run they are transferred one at a time and positioned exactly in the center of the deposition chamber. The Argon pressure during the deposition is precisely fixed and monitored to a value of 4×10^{-3} mbar. The Nb and PdNi layers have been deposited at typical power of $W_{Nb}=77$ Watt and $W_{PdNi}=105$ Watt, which correspond to the rates $r_{Nb}=1$ Å/s and $r_{PdNi}=2$ Å/s, respectively. This careful deposition procedure is necessary to exclude fluctuations of the samples parameters.

2.2. Compositional analysis. Superconducting and magnetic properties

Since the ferromagnetic properties of the PdNi alloy strongly depends on the Ni content a careful characterization of this quantity is necessary. To this purpose the Ni concentration in the samples was checked by Energy Dispersive Spectroscopy (EDS). In particular, to determine the Ni content and the uniformity of the composition the samples were analysed using a LEO-EVO 50 scanning electron microscope equipped with an energy dispersive spectrometer (EDS, Oxford INCA Energy 300). The EDS analysis was performed over different areas for each film. This investigation pointed out a uniform percentage of Ni in PdNi alloy. The result of both the methods gives the value of 19% for Ni in PdNi alloy which is well above the critical percentage [39].

The superconducting and magnetic properties of the Nb/PdNi multilayers have been studied in great details in previous papers [40–42]. Here in Fig. 1 we show the resistive transition curve for the sample KL5, which becomes superconducting at $T=5.5$ K.

Using a Vibrating Sample Magnetometer (Cryogenics Ltd.), magnetization curves have been measured to observe if magnetism was established in the hybrids. Due to the small signal coming from the thin layers of the weakly ferromagnetic alloy a multilayer with $m=14$ has been deliberately fabricated in order to increase the magnetic signal. In Fig. 2 is plotted the $M(H)$ curve measured on this multilayer which shows that at $T=4$ K the sample is ferromagnetic. From that, we calculated the saturation magnetization $M_{sat}=0.33\ \mu_B$/atom. This value agrees with the one obtained using a SQUID magnetometer on a single PdNi film (19.2 nm thick) with the same Ni content [40].

3. Low angle X-ray reflectometry

3.1. The scattering geometry

A Philips X'Pert-MRD high resolution analytic diffractometer equipped with a four-circle cradle was used to study the X-ray reflectivity of the samples. A Cu $K_{\alpha1}$ ($\lambda=1.5406$ Å) source was used at 40 kV and 40 mA. Low angle X-ray measurements were carried out by using a monochromatic radiation obtained equipping the diffractometer with a four crystal Ge 220 Bartels asymmetric monochromator and a graded parabolic Guttman mirror positioned on the primary arm. On the secondary arm, a parallel thin film collimator guaranteed the alignment of the reflected beam from the samples to the detector.

In Fig. 3 is shown a schematic drawing of coplanar X-ray reflectivity measurements performed in the present experiment. The incident angle, ω, is the angle at which the X-ray beam falls on the sample surface. The angle between the incident beam and the diffracted beam is indicated as 2θ. The scattering process involves the wave vectors of the incident and the scattered wave, $\mathbf{q}_i$ and $\mathbf{q}_f$ respectively, defining the wave vector transfer $\mathbf{q}=\mathbf{q}_i-\mathbf{q}_f$. The angular coordinates are related to wave vector transfer ones according to:

$$q_x = \frac{2\pi}{\lambda}(\cos\omega - \cos(2\theta-\omega))$$

$$q_z = \frac{2\pi}{\lambda}(\sin\omega + \sin(2\theta-\omega))$$

representing the components of the wave vector transfer parallel and perpendicular to the scattering plane. In this way it separates regions

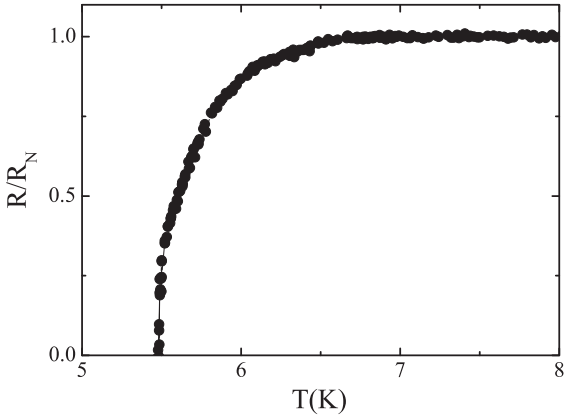

Fig. 1. Superconducting transition curve for the sample KL5.

Библиотека БГУИР

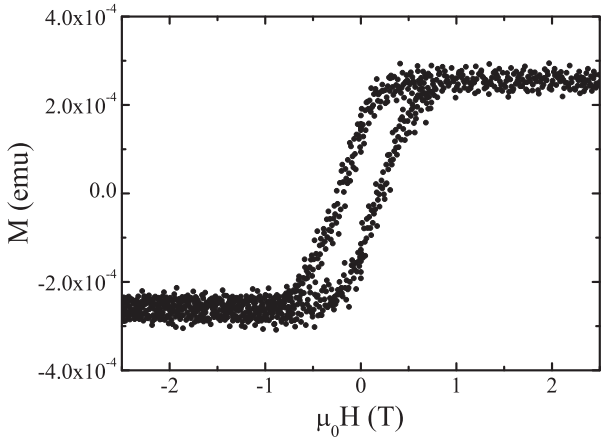

Fig. 2. Magnetization curve at T = 4 K for a Nb/PdNi multilayer with $m = 14$.

of the reciprocal space which are accessible with different scattering techniques. The region close to $\mathbf{q} \approx 0$ is the reflectivity region; the specular part [$q_x = 0$, $q_z \neq 0$)] is governed by the Fresnel laws, while the non-specular reflectivity region [$q_x \neq 0$, $q_z \neq 0$] is governed by elastic diffuse scattering. For higher wave vector transfer satisfying the conditions [$q_x = 0$, $q_z \geq q_{zB}$] or [$q_x \neq 0$, $q_z \geq q_{zB}$] it gets into the region where the extended reflectivity has to be taken into account. Here, q_{zB} is the wave vector related to the Bragg reflection with the lowest Miller index. This region will be not analyzed in the present experiment. In the reciprocal space, the scattering wave vectors $\mathbf{q}_f$ which are accessible for a flat sample are shown in Fig. 3. There are also two inaccessible semicircular regions corresponding to areas where either the incident beam or the diffracted beam are below the horizon of the sample.

3.2. Specular X-ray reflectivity

The reciprocal space of a perfect multilayer within the region of specular reflectivity is made of equidistant points along the q_z axis, the so-called Bragg-like reflections. Their spacing $\Lambda_1 = q_{z_j} - q_{z_{j-1}} = \frac{2\pi}{d}$, $j \geq 2$ being an integer, is inversely proportional to the super-period $d = d_{Nb} + d_{PdNi}$ of the multilayer. The intensity of the Bragg-like reflections can be modulated by additional maxima between them, known as Kiessig fringes [43]. In our case, *m-1* (with $m = 5, 7, 9$) maxima in between two Bragg-like reflections for a sample with m Nb/PdNi bilayers can be expected. These maxima are spaced by $\Lambda_2 = q_{z_k} - q_{z_{k-1}} = \frac{2\pi}{t}$, with $k = 2, \ldots, m$ and t representing the whole sample thickness. In Fig. 4 we show the specular X-ray reflectivity patterns of the multilayers with $m = 5$ (sample KL5, panel a), $m = 7$ (sample KL7, panel b) and $m = 9$ (sample KL9, panel c).

The wave vector at which the X-rays intensity starts to drop off represents the critical wave vector, q_{z_c}, related to the total reflection of the X-rays (for $q < q_{z_c}$) and electron density of the uppermost layer.

As the wave vector increases ($q > q_{z_c}$), the X-rays start to penetrate into the samples instead of reflecting off on it. When the incident beam penetrates all the way through the samples to either the substrate or the next layer down, Bragg-like reflections are observable. The main periodic Bragg-like reflections demonstrate the good stratification of

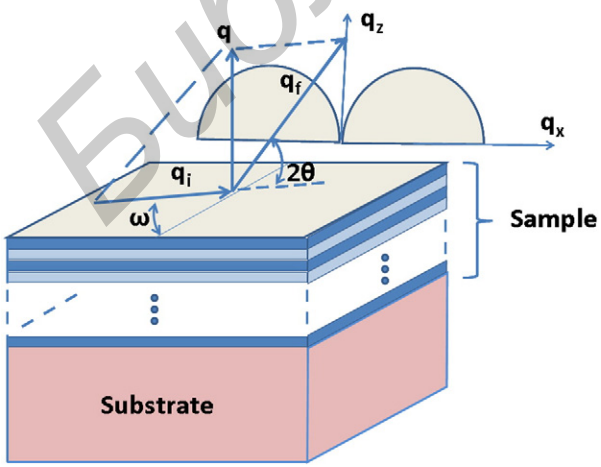

Fig. 3. Scattering geometry; ω is the incident angle, 2θ is the scattered angle. The wave vector transfer $\mathbf{q} = \mathbf{q}_f - \mathbf{q}_i$ is also drawn.

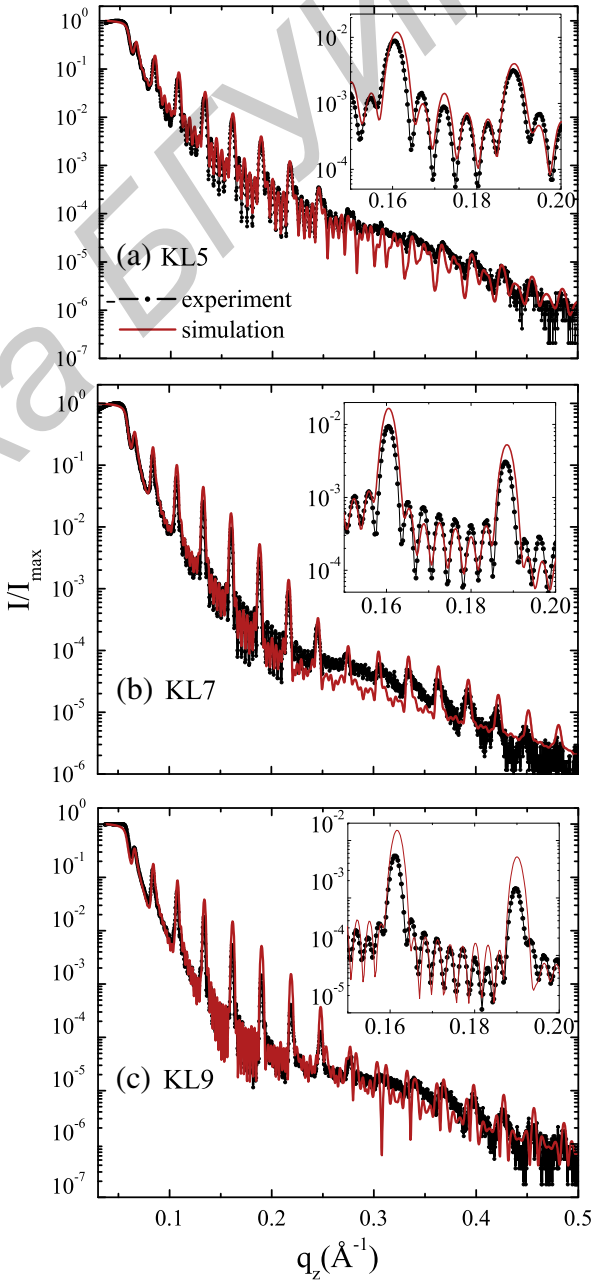

Fig. 4. Experimental (black line and scatter) and calculated (red line) specular reflectivities of the different multilayers: (a) KL5, (b) KL7, and (c) KL9. Insets: enlargements of the spectra showing Bragg-like reflections and Kiessig fringes due to the multilayers periodicity.

Библиотека БГУИР

the samples with a defined modulation wavelength associated with the multilayered structure. At the first Bragg-like order, the bandpass of the multilayers is proportionally more pronounced for the KL9 sample (37%) compared with KL5 (34%) and KL7 (30%) ones. From a comparison among the X-ray reflectivity patterns, the progressive damping of the scattered intensity is slightly weaker for KL7 sample with respect KL5 and KL9 samples. This is an indication that for the sample KL7 the interfaces are, in average, less rough. From Fig. 4, the large number of very well identified and regularly spaced Kiessig fringes (see the insets) between two neighboring Bragg-like ones, with pronounced peaks and valleys, gives clear evidence for defined interfaces through the different layers. The patterns show the number *m-1* of diffraction orders expected from samples with $m=5$, 7 and 9, respectively. Their positions and amplitudes are related to the whole sample thickness and to the surface roughness. From the spacing in q_z of the Kiessig fringes the total multilayers thickness can be determined by fitting procedures. The simulation curves reported in Fig. 4 were obtained with the Parratt algorithm [44] taking roughness into account according to Nevot and Croce [45]. Within the fit procedure, the roughness of each single layer was supposed to be independent on the roughness of other layers (the case of uncorrelated roughness). As it can be observed, the agreement between the fit procedure and the experimental patterns is excellent up to higher measured wave vectors transfer. The fit gives the mean thickness of the single layers as well as the value of the sample roughness (see Table 1). In the framework of the fitting model, we deduce that the thickness of Nb and PdNi layers is constant in the multilayer structure, while the values of the root-mean-square roughness, σ, are in general smaller for the internal layers (4–8 Å) and larger for the bottom and the capping layers (8–11 Å). The distribution of the roughness of the single layers in the samples as resulted by the fitting procedure, is shown in Fig. 5. These results point out that the layering quality of the samples does not depend on *m*. The obtained values listed in Table 1 for the thickness of the Nb and PdNi layers are in excellent agreement with the nominal ones estimated by measuring the deposition time during the growth. Moreover, the KL7 sample shows the smoother average roughness at the interfaces as already suggested by the damping of X-ray reflectivity patterns seen above.

3.3. Diffuse X-ray reflectivity

The diffuse X-ray reflectivity depends on in-plane component, q_x, of the wave vector transfer and brings information on the details of the lateral ordering of the interface roughness profiles [46] as well as the vertical replications of the roughness from one interface to another of the multilayers. These unique information are relevant for the properties of the multilayers and also for the feedback on the growth process itself.

Experimentally, the X-ray reflectivity reciprocal space map in the region $[q_x \neq 0, q_z \neq 0]$ is the proper tool to study the main features of the interfacial roughness. As an example, Fig. 6 shows the X-ray reflectivity reciprocal space map of the sample KL9. The vertical rod in the Fig. 6 is the specular one corresponding to $q_x \sim 0$. A set of Bragg-like spots appear along the specular line at $q_z = n\Lambda_1$, n being an integer, the order of Bragg-like diffraction. Moreover, Kiessig spots at

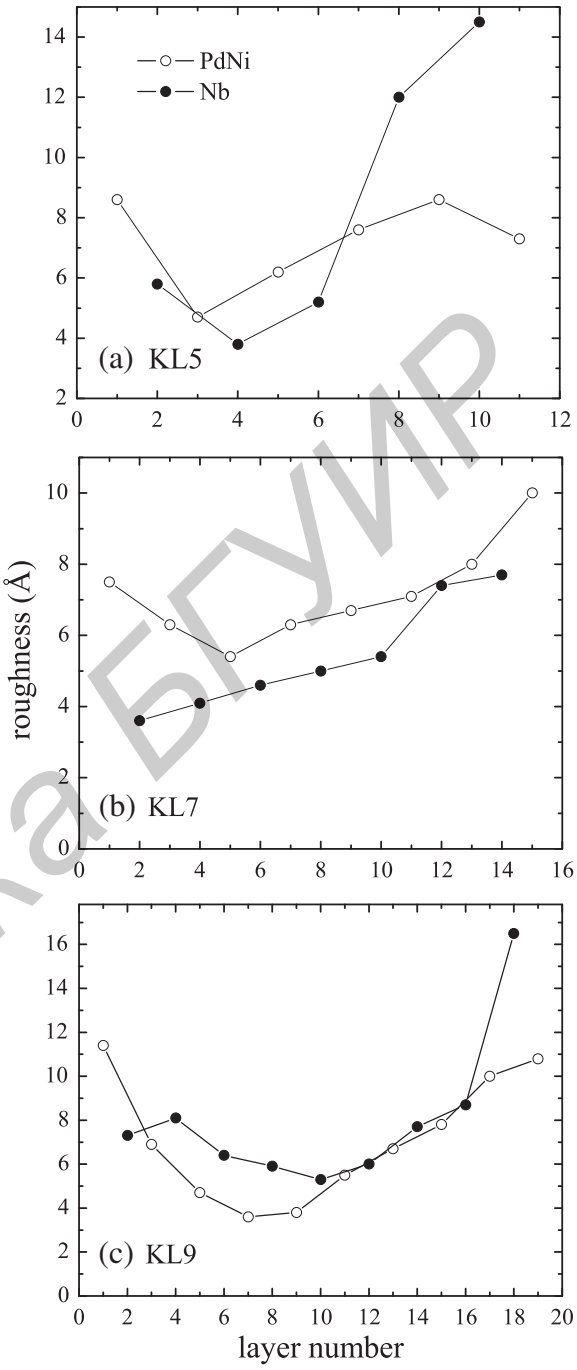

Fig. 5. The PdNi (open symbols) and Nb (closed symbols) layer roughness as a function of the layer number for the different multilayers: (a) KL5, (b) KL7, and (c) KL9.

$q_z = k_m \Lambda_2$ (where k_m is an integer) in between the Bragg-like spots are observable.

Each Bragg-like spot is crossed by a diffuse line that extends along the lateral q_x direction; many lines are observed in our samples. These structures correspond to the so-called Bragg stripes arising from the resonant diffuse scattering [47]. As a function of the degree of vertical replication of the thickness fluctuations from layer to layer, various cases with specific scattering behaviors can be identified: perfectly smooth interfaces (no roughness), perfect replication with intrinsic roughness (identical interfaces), fully uncorrelated roughnesses (no replication), and partially correlated interfaces [47,48]. For uncorrelated layers, the diffuse scattering is the incoherent sum of the scattering from individual layers added to the specular rod.

Table 1
Samples parameters obtained from the simulation of the experimental XRR patterns of the three analyzed multilayers. Here m is the number of period in the structures, d_{Nb} and d_{PdNi} are the thickness of the Nb and the PdNi layers, respectively. The average values of the roughness corresponding to each layer is also indicated.

m	dNb(Å)	σNb(Å)	dPdNi(Å)	σPdNi(Å)
5	187.4	8.3	22.0	7.2
7	187.1	8.0	23.3	7.1
9	187.1	5.4	20.8	7.2

Библиотека БГУИР

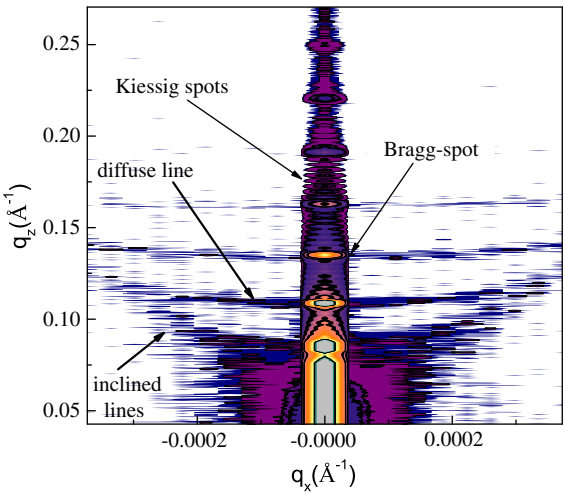

Fig. 6. Reciprocal space reflectivity map of the multilayer KL9.

The intensity is therefore spread in the reciprocal space. From the shown measurements, it can be deduced that our multilayers have an interfacial roughness that is partially correlated from one layer to another. This is testified by the occurrence of such Bragg stripes in the reported reciprocal space maps centered on the Bragg-like spots with diffuse scattered intensity along the q_x direction [46,49]. Because of beam refraction [47], these stripes are curved in the [q_x, q_z] plane giving rise to the so-called "bananas" structures [47].

The q_z width, Δq_z, at a given q_x characterizes the decay length of the cross correlation between interfaces for a given spatial wavelength. Thus, their q_z spread is related to the degree of roughness replication i.e. to the inverse of the cross correlation length [49,50]. The Bragg stripes have finite thickness q_z given approximately by $\Delta q_z = \frac{2\pi n}{dm^*}$, where m^* is the effective number of bilayers over which the roughness is correlated [50]. In the case of fully correlated roughness, $m^* = m$ is the whole number of Nb/PdNi bilayers of the samples.

From the measurement of the width of the Bragg stripes, one can estimate $m^* = 9$ for the sample KL9. Analogously, from the reflectivity space maps, $m^* = 5$ and $m^* = 7$ was obtained from KL5 and KL7 samples, respectively. The estimations reported above point out that the samples have at least a strong correlated roughness or, as extreme case, a complete correlation. Finally, in addition to the Bragg-like spots and Bragg stripes, one can observe, symmetrically about the specular line, some inclined lines emerging from the Bragg-like spots of lowest orders (see Fig. 6). Their origin may be attributed to dynamically resonant effects of multiple specular reflection and extinction of the scattered radiation [47].

4. Conclusions

In conclusion, high-quality Nb/PdNi multilayers having both superconducting and ferromagnetic orders and prepared by UHV sputtering, show interesting structural features that can be interpreted in terms of typical coherent and diffuse scattering processes. X-ray diffraction measurements are useful to determine structural properties of these hybrids. In particular, the average roughness of each layer has been evaluated and numbers are smaller for the internal layers and larger for the top and bottom ones. Diffuse X-ray reflectivity spectra indicate that roughness is highly correlated along the different layers and preserved up to $m = 9$. Our study shows that Nb/PdNi multilayers present good layering properties which are crucial in view of possible applications of this kind of structures in the field of spintronics and superconducting electronics [1,51].

Acknowledgments

The authors wish to thank A.I. Akimov for magnetic measurements and A. Guarino for fruitful scientific discussion. This work has been partially supported by the Belarus Foundation for Fundamental Research, project F10R-063 (S.L.P. and V.N.K.) and by the Russian Foundation for Fundamental Research project # 10-02-90014-Bel-a (M.Yu.K.). The research leading to these results has received funding from the European Union Seventh Framework Programme (FP7/2007-2013) under grant agreement N. 264098 – MAMA (R.F).

References

[1] A.I. Buzdin, Rev. Mod. Phys. 77 (2005) 935.
[2] F.S. Bergeret, A.F. Volkov, K.B. Efetov, Rev. Mod. Phys. 77 (2005) 1321.
[3] I.A. Garifullin, J. Magn. Magn. Mater. 240 (2002) 571.
[4] C. Cirillo, C. Bell, G. Iannone, S.L. Prischepa, J. Aarts, C. Attanasio, Phys. Rev. B 80 (2009) 094510.
[5] V.V. Ryazanov, V.A. Oboznov, A.Yu. Rusanov, A.V. Veretennikov, A.A. Golubov, J. Aarts, Phys. Rev. Lett. 86 (2001) 2427.
[6] A.A. Golubov, M.Yu Kupriyanov, E. Il'ichev, Rev. Mod. Phys. 76 (2004) 411.
[7] T. Kontos, M. Aprili, J. Lesueur, X. Grison, Phys. Rev. Lett. 86 (2001) 304.
[8] H.K. Wong, B.Y. Jin, H.Q. Yang, J.B. Ketterson, J.E. Hilliard, J. Low Temp. Phys. 63 (1986) 307.
[9] J.S. Jiang, D. Davidović, D.H. Reich, C.L. Chien, Phys. Rev. Lett. 74 (1995) 314.
[10] J.E. Mattson, C.D. Potter, M.J. Conover, C.H. Sowers, S.D. Bader, Phys. Rev. B 55 (1997) 70.
[11] G. Verbanck, C.D. Potter, V. Metlushko, R. Schad, V.V. Moshchalkov, Y. Bruynseraede, Phys. Rev. B 57 (1998) 6029.
[12] P. Koorevaar, Y. Suzuki, R. Coehoorn, J. Aarts, Phys. Rev. B 49 (1994) 441.
[13] C. Strunk, C. Sürgers, U. Paschen, H.v. Löhneysen, Phys. Rev. B 49 (1994) 4053.
[14] Th. Mühge, N.N. Garifyanov, Yu.V. Goryunov, G.G. Khaliullin, L.R. Tagirov, K. Westerholt, I.A. Garifullin, H. Zabel, Phys. Rev. Lett. 77 (1996) 1857.
[15] A.S. Sidorenko, V.I. Zdravkov, A.A. Prepelitsa, C. Helbig, Y. Luo, S. Gsell, M. Schreck, S. Klimm, S. Horn, L.R. Tagirov, R. Tidecks, Ann. Phys. 12 (2003) 37.
[16] V. Zdravkov, A. Sidorenko, G. Obermeier, S. Gsell, M. Schreck, C. Muüller, S. Horn, R. Tidecks, L.R. Tagirov, Phys. Rev. Lett. 97 (2006) 057004.
[17] A.S. Sidorenko, V.I. Zdravkov, J. Kehrle, R. Morari, G. Obermeier, S. Gsell, M. Schreck, C. Müller, M.Yu. Kupriyanov, V.V. Ryazanov, S. Horn, L.R. Tagirov, R. Tidecks, Pis'ma v ZhETP 90 (2009) 149;
JETP Lett. 90 (2009) 139.
[18] Z.C. Dong, D.Y. Xing, J. Dong, J. Phys. Condens. Matter 13 (2001) 3839.
[19] M. Weides, K. Tillmann, H. Kohlstedt, Physica C 437–438 (2006) 349.
[20] M. Weides, M. Kemmler, E. Goldobin, D. Koelle, R. Kleiner, H. Kohlstedt, A. Buzdin, Appl. Phys. Lett. 89 (2006) 122511.
[21] B.P. Vodopyanov, L.R. Tagirov, H.Z. Durusoy, A.V. Berezhnov, Physica C 366 (2001) 31.
[22] I.A. Garifullin, N.N. Garifyanov, R.I. Salikhov, Bull. Russ. Acad. Sci: Physics 71 (2007) 272.
[23] M. Weides, M. Kemmler, H. Kohlstedt, R. Waser, D. Koelle, R. Kleiner, E. Goldobin, Phys. Rev. Lett. 97 (2006) 247001;
M. Kemmler, M. Weides, M. Weiler, S.T.B. Goennenwein, A.S. Vasenko, A.A. Golubov, H. Kohlstedt, D. Koelle, R. Kleiner, E. Goldobin, Phys. Rev. B 81 (2010) 054522.
[24] Trupti S. Khaire, Mazin A. Khasawneh, W.P. Pratt Jr., Norman O. Birge, Phys. Rev. Lett. 104 (2010) 137002.
[25] Mazin A. Khasawneh, Trupti S. Khaire, Klose Carolin, William P. Pratt Jr., Norman O. Birge, Supercond. Sci. Technol. 24 (2011) 024005.
[26] S.L. Prischepa, C. Cirillo, C. Bell, V.N. Kushnir, J. Aarts, C. Attanasio, M.Yu. Kupriyanov, Pis'ma v ZhETF 88 (2008) 431;
JETP Lett. 88 (2008) 375.
[27] V.N. Kushnir, S.L. Prischepa, J. Aarts, C. Bell, C. Cirillo, C. Attanasio, Eur. Phys. J. B 80 (2011) 445.
[28] V.N. Kushnir, S.L. Prischepa, C. Cirillo, C. Attanasio, A. Vecchione, M. Yu. Kupriyanov, J. Aarts, Phys. Rev. B, submitted for publication.
[29] L. Soriano, M. Sánchez-Agudo, R.J.O. Mossanek, M. Abbate, G.G. Fuentes, P.R. Bressler, L. Alvarez, J. Méndez, A. Gutiérrez, Surf. Sci. 605 (2011) 539.
[30] S.D. Bader, Surf. Sci. 500 (2002) 172.
[31] G. Palasantzas, J.Th.M. De Hosson, J. Barnas, Surf. Sci. 507–510 (2002) 541.
[32] W.P. Lowe, T.W. Barbee Jr., T.H. Geballe, D.B. McWhan, Phys. Rev. B 24 (1981) 6193.
[33] C. Gerardi, M.A. Tagliente, A. Del Vecchio, L. Tapfer, C. Coccorese, C. Attanasio, L.V. Mercaldo, L. Maritato, J.M. Slaughter, C.M. Falco, J. Appl. Phys. 87 (2000) 717.
[34] W.P. Lowe, T.H. Geballe, Phys. Rev. B 29 (1984) 4961.
[35] Th. Mühge, K. Theis-Bröhl, K. Westerholt, H. Zabel, N.N. Garifyanov, Yu.V. Goryunov, I.A. Garifullin, G.G. Khaliullin, Phys. Rev. B 57 (1998) 5071.
[36] M. Velez, M.C. Cyrille, S. Kim, J.L. Vicent, I.K. Schuller, Phys. Rev. B 59 (1999) 14659.
[37] Y. Obi, M. Ikebe, H. Fujishiro, Phys. Rev. Lett. 94 (2005) 057008.

Библиотека БГУИР

[38] E. Navarro, J.E. Villegas, J.L. Vincent, J. Magn. Magn. Mater. 240 (2002) 586.
[39] G.J. Nieuwenhuys, Adv. Phys. 24 (1975) 515.
[40] C. Cirillo, A. Rusanov, C. Bell, J. Aarts, Phys. Rev. B 75 (2007) 174510.
[41] C. Cirillo, S.L. Prischepa, M. Salvato, C. Attanasio, M. Hesselberth, J. Aarts, Phys. Rev. B 72 (2005) 144511.
[42] G. Iannone, D. Zola, A. Angrisani Armenio, M. Polichetti, C. Attanasio, Phys. Rev. B 75 (2007) 064409.
[43] H. Kiessig, Ann. Phys. Leipzig 10 (1931) 769.
[44] L.G. Parratt, Phys. Rev. 95 (1954) 359.
[45] L. Nevot, P. Croce, Rev. Phys. Appl. 15 (1980) 761.
[46] D.E. Savage, J. Kleiner, N. Schimke, Y.H. Phang, T. Jankowski, J. Jacobs, R. Kariotis, M.G. Lagally, J. Appl. Phys. 69 (1991) 1411.
[47] V. Holy, T. Baumbach, Phys. Rev. B 49 (1994) 10668.
[48] A.P. Payne, B.M. Clemens, Phys. Rev. B 47 (1993) 2289.
[49] T. Salditt, D. Lott, T.H. Metzger, J. Peisl, G. Vignaud, P. Høghøj, O. Schärpf, P. Hinze, R. Lauer, Phys. Rev. B 54 (1996) 5860.
[50] D.G. Stearns, J. Appl. Phys. 71 (1992) 4286.
[51] M.I. Khabipov, D.V. Balashov, F. Maibaum, A.B. Zorin, V.A. Oboznov, V.V. Bolginov, A.N. Rossolenko, V.V. Ryazanov, Supercond. Sci. Technol. 23 (2010) 045032.

Библиотека БГУИР